Bioactive Materials 34 (2024) 326–337

Contents lists available at ScienceDirect

Bioactive Materials

journal homepage: www.keaipublishing.com/en/journals/bioactive-materials

Intracellular and extracellular synergistic therapy for restoring macrophage functions via anti-CD47 antibody-conjugated bifunctional nanoparticles in atherosclerosis

Qiang Luo [a,1], Liqun Dai [b,1], Junli Li [a], Heyanni Chen [c], Ying Hao [a], Qing Li [a], Lili Pan [d], Chengxiang Song [a], Zhiyong Qian [b,*], Mao Chen [a,**]

[a] Laboratory of Heart Valve Disease, West China Hospital, Sichuan University, #37 Guoxue Alley, Chengdu, 610064, China
[b] State Key Laboratory of Biotherapy and Cancer Center, West China Hospital, West China Medical School, Sichuan University, Collaborative Innovation Center of Biotherapy, Chengdu, 610041, China
[c] West China Medical School, Sichuan University, Chengdu, 610041, Sichuan, China
[d] Department of Nuclear Medicine, Laboratory of Clinical Nuclear Medicine, West China Hospital, Sichuan University, Chengdu, 610041, Sichuan, China

ARTICLE INFO

Keywords:
Anti-CD47
Atherosclerosis
Bifunctional
Anti-inflammation
NLRP3

ABSTRACT

Atherosclerosis is a significant contributor to global cardiovascular disease. Reducing the formation of atherosclerotic plaque effectively can lead to a decrease in cardiovascular diseases. Therefore, controlling macrophage function is crucial. This study presents the creation of a bifunctional nanoparticle that is specific to macrophages to achieve intracellular and extracellular synergistic therapy for restoring macrophage functions. The nanoparticle is conjugated with anti-CD47 antibody to modulate extracellular CD47-SIRPα phagocytic signaling axis on the outer surface of macrophages and encapsulates the NLRP3 inhibitor (CY-09) to regulate intracellular inflammation response of macrophages. The results showed that the nanoparticles accumulate in the atherosclerotic plaque, alter macrophage phagocytosis, inhibit NLRP3 inflammasome activation, and decrease the plaque burden in Apoe$^{-/-}$ mice whilst ensuring safety. Examination of single-cell RNA sequencing indicates that this multifunctional nanoparticle decreases the expression of genes linked to inflammation and manages inflammatory pathways in the plaque lesion. This study proposes a synergistic therapeutic approach that utilizes a bifunctional nanoparticle, conjugated with anti-CD47, to regulate the microenvironment of plaques.

1. Introduction

Macrophages play a pivotal role in the development of atherosclerotic plaque, making their regulation an essential target for treating atherosclerosis [1–4]. Previous research has indicated that diseased vascular endothelial cells and apoptotic debris accumulation in the subintima characterize atheromatous plaques [5]. Additional research has shown that the signal regulatory protein-α (SIRPα) present on the surface of macrophages could interact with the CD47, a protein expressed on the surface of apoptotic cells in atherosclerotic plaques. This interaction disrupts the phagocytic signaling, hindering the macrophages' ability to clear pathological and apoptotic cells (Fig. 1A) [6–8]. To counteract this CD47-SIRPα anti-phagocytic signaling axis, researchers injected an anti-CD47 monoclonal antibody into mouse models of atherosclerosis. This intervention with anti-CD47 antibody led to enhanced clearance of apoptotic cells and a significant reduction in atherosclerotic plaque size, demonstrating its potential as a promising therapeutic agent in the treatment of atheromatous plaques [6].

In addition, it was found that the blockade of CD47 could ameliorate the production of NLRP3 inflammasome-induced IL-1β, a key inflammatory cytokine [9,10]. Beyond aberrant phagocytosis, the macrophage-initiated inflammatory response plays a substantial role in the development of atherosclerotic plaques [11–13]. Macrophages activate the NLRP3 inflammasome upon internalizing oxidized

Peer review under responsibility of KeAi Communications Co., Ltd.
* Corresponding author.
** Corresponding author.
E-mail addresses: anderson-qian@163.com (Z. Qian), chenmao@scu.edu.cn (M. Chen).
[1] These two authors contributed equally to this work.

https://doi.org/10.1016/j.bioactmat.2023.12.024
Received 24 October 2023; Received in revised form 27 December 2023; Accepted 27 December 2023

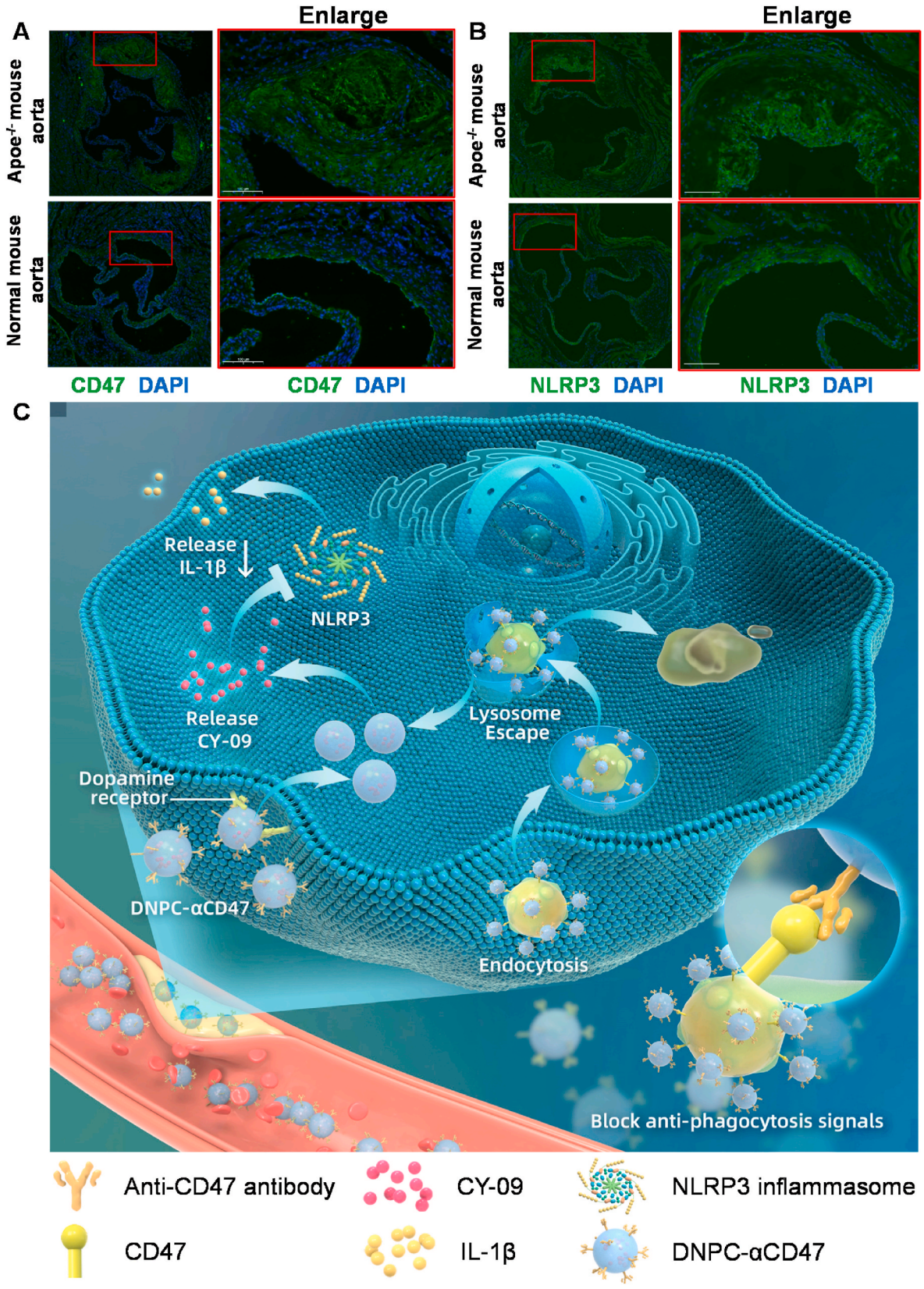

Fig. 1. A, The higher expression of CD47 in atherosclerotic model mouse than normal mouse aorta via immunofluorescence (Scale bar: 100 μm); **B,** The higher expression of NLRP3 in atherosclerotic model mouse than normal mouse aorta via immunofluorescence (Scale bar: 100 μm); **C,** Schematic illustration of the bifunctional nanoparticle formula and the application in chronic atherosclerotic mouse model.

low-density lipoprotein (ox-LDL). This activation results in substantial secretion of the inflammatory factor IL-1β (Fig. 1B) [14], promoting tissue damage and the formation of atherosclerotic lesions. Given the central role of the NLRP3 inflammasome in this process, targeting it offers a promising approach to atherosclerosis therapy.

Nanoscale drug delivery systems, commonly used in treating tumors, offer a dual solution to both anti-phagocytosis and anti-inflammation challenges in atherosclerotic plaques. These systems are particularly effective due to their ability to passively target specific cells and their multifunctional properties [15–18]. In atherosclerotic diseases, chronic inflammation results in increased permeability of vascular endothelial cells, facilitating the accumulation of nanoparticles at the plaque sites through the enhanced permeability and retention (EPR) effect [19,20]. Enhanced therapeutic effects and reduced systemic side effects are observed simultaneously with high nanoparticle accumulation within the plaque. We hypothesized that conjugating monoclonal antibodies onto nanoparticle surfaces can enable targeted delivery of antibodies to the plaque site while minimizing systemic side effects. Moreover, antibody-conjugated nanoparticles can encapsulate small-molecule drugs to achieve drug delivery in addition to antibody delivery. In this study, we encapsulated CY-09, a novel NLRP3 inflammasome inhibitor, to suppress the assembly and activation of the NLRP3 inflammasome. Furthermore, the delivery of encapsulated NLRP3 inhibitors can remodel the inflammatory microenvironment of macrophages in addition to resolving issues caused by anti-CD47 monoclonal antibodies.

Furthermore, the efficiency of drug delivery using nanoscale delivery systems is crucial. The efficiency of transporting nanoparticles greatly relies on their capacity to escape the lysosome [21]. Upon entering the cell, the nanoparticles become enclosed by membrane vesicles and transported to the lysosome. Once there, they should be able to successfully break the lysosome and deliver the payload to the cytoplasm, thus safeguarding the payloads from degradation by various digestive enzymes present in the lysosome [22,23]. Previous research has shown that phenylboronic acid facilitates lysosome escape and supports transcellular agent transfer [24,25]. Thus, for this study, polydopamine nanoparticles (DNP) were produced using a one-step process that relied on the interaction between boronic acid in boronophenylalanine (BPA) and the phenolic hydroxy group of dopamine. Polydopamine nanoparticles are commonly used polymers in the nanomedicine field due to their excellent biocompatibility and adhesion [26–31].

Here, we describe a novel therapy for atherosclerosis using a functional polydopamine-phenylboronic acid nanomedicine conjugated with anti-CD47 antibodies. Our approach simultaneously targets phagocytosis restoration and inflammation inhibition (Fig. 1C). Initially, we utilized hydrophobic forces to encapsulate CY-09 within nanoparticles. Following this, we determined the optimal nanoparticle-to-antibody ratio. In vitro cell experiments suggest that this two-pronged nanoparticle effectively impedes reactive phagocytosis of macrophages and NLRP3 inflammasome activation. In vivo animal studies indicate that these nanoparticles can considerably reduce plaque burden without any associated toxicity. This bifunctional nanoparticle offers valuable insights into the development of synergistic nanomedicines for atherosclerosis therapy.

2. Results

2.1. Preparation and characterization of bifunctional nanoparticles

In this work, polydopamine nanoparticles (DNPs) were prepared via a one-step process based on the interactions between the boronic acid of boronophenylalanine (BPA) and the phenolic hydroxy group of dopamine. DNPs were easily fabricated by encapsulating BPA in polydopamine via nitrogen-boronate coordination. The NLRP3 inhibitor, CY-09, was loaded into DNP by overnight stirring to obtain DNPC nanoparticles, and the excess free drug was removed by centrifugation. Furthermore, the anti-CD47 antibody was conjugated to the surface of DNPC by covalent linkage via a Schiff reaction, and DNPC-αCD47 was obtained (Fig. 2A). The size and zeta potential of DNP, DNPC, and DNPC-αCD47 were characterized by dynamic light scattering (DLS). In aqueous solution, DNP and DNPC nanoparticles have a narrow size distribution with a mean particle size of 190 nm (PDI of 0.10) and 193 nm (PDI of 0.07), respectively. After the conjugation of αCD47, the hydrated particle size of DNPC-αCD47 increased to 320 nm (PDI of 0.15) (Fig. 2B), indicating that the antibody was successfully conjugated on the surface of nanoparticles. DLS showed that the zeta potentials of DNP, DNPC and DNPC-αCD47 were -45 ± 0.53 mV, -32 ± 0.48 mV and -35 ± 0.42 mV, respectively (Fig. 2C). The negative charge on the surface of the nanoparticles can reduce the adsorption of proteins in the blood and increase circulatory stability. In addition, these nanoparticles have good particle size and potential stability. As shown in Fig. 2D, no obvious change in particle size and zeta potential was detected in DNPC-αCD47 during 24 h at 37 °C in PBS. To further explore the particle size and morphology of nanoparticles, TEM images of three nanoparticles were acquired in the dry phase, as shown in Fig. 2E–G. From the results, the particle size of DNPC-αCD47 nanoparticles was similar to DNP and DNPC (about 190 nm). Besides, the blurred outline on the surface indicated that a layer of protein was attached to the nanoparticle (Fig. 2G). To determine the optimal conjugation ratio, different conjugation ratios were performed by adjusting the ratio of nanoparticles to antibodies (Table S1). From these results, the 1:1 nanoparticle to antibody ratio was selected as the final ratio with a 94 % conjugation rate. To further verify the antibody conjugation, a significant lane was detected at 25–50 KDa after Coomassie blue staining of SDS-PAGE gel electrophoresis. The protein lane in DNPC-αCD47 is the same as the free anti-CD47 antibody, which also indicates that the anti-CD47 antibody was successfully conjugated on the surface of nanoparticles (Fig. 2J). Moreover, the encapsulation of CY-09 in DNPC was detected by UV spectroscopy as shown in Fig. 2H. From this result, a 380 nm peak was clearly detected in the UV spectra of DNPC compared to DNP nanoparticles. The release of CY-09 in DNPC was also tested by high-performance liquid chromatography (HPLC). CY-09 can release approximately 60 % in 12 h in PBS at 37 °C (Fig. 2I). The release profile of CY-09 in DNPC-αCD47 is similar to DNPC. Based on these results, anti-CD47 antibody conjugated and CY-09 encapsulated polydopamine-based nanoparticles with suitable particle size and potential and good stability were successfully prepared.

2.2. Cellular uptake, lysosome escape, and endocytic pathway

To study the cellular uptake and follow the endocytic pathways of the nanoparticles, chlorin e6 (Ce6) was also encapsulated in DNPC-αCD47 nanoparticles as a fluorescent probe. The cellular uptake of DNPC-αCD47 by RAW264.7 cells was examined by flow cytometry as shown in Fig. 3A–B. As the incubation time or nanoparticle concentration increased, the fluorescence intensity in the cells increased, indicating that the number of nanoparticles internalized by the cells also increased significantly. This suggests that DNPC-αCD47 nanoparticles can be rapidly and easily taken up by macrophages. The endocytic pathways for these polymers were then investigated. Cells were co-incubated with different endocytic markers labeled with Alexa-Fluor®488 and DNPC-αCD47. Fluorescence images showed that DNPC-αCD47 nanoparticles co-localized with cholera toxin subunit B, a marker of caveolae-mediated endocytosis, but not with dextran or transferrin, markers of micropinocytosis or clathrin-mediated endocytosis, as shown in Fig. 3C [15,18]. Furthermore, co-incubation of free dopamine and DNPC-αCD47 nanoparticles can significantly reduce the uptake of nanoparticles by macrophages, indicating that dopamine receptor-mediated endocytosis plays an important role in the uptake of nanoparticles (Fig. 3D). Upon entering the cell, the nanoparticles are internalized by membrane vesicles and transported to the lysosome. The efficiency of transporting nanoparticles greatly relies on their capacity to escape the lysosome. The lysosome escape of nanoparticles was

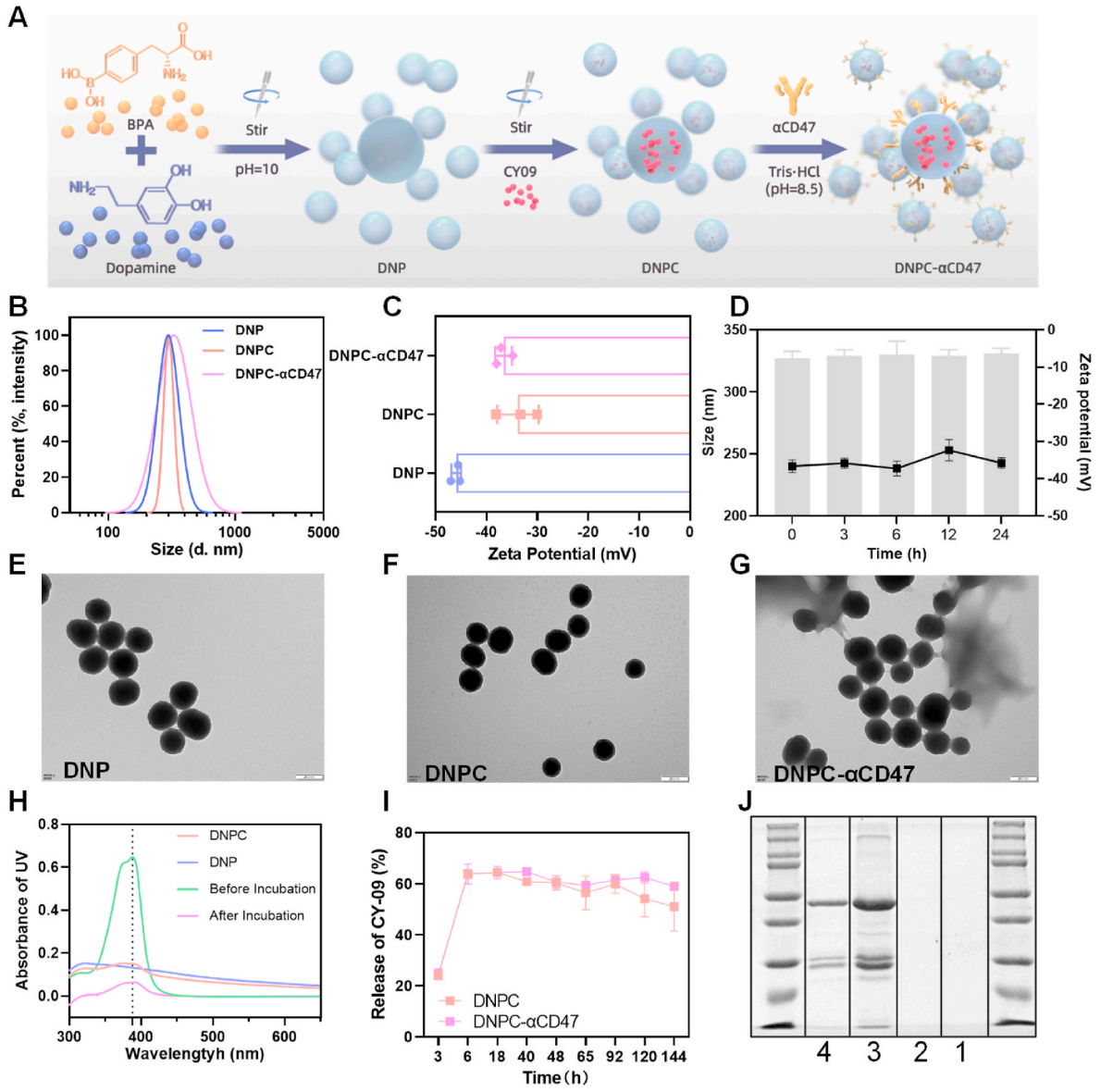

Fig. 2. A, Schematic illustration of the preparation of DNP, DNPC and DNPC-αCD47 nanoparticles; **B–C**, Size and zeta potentials of nanoparticles; **D,** Stability of size and zeta potentials in 24 h; **E-G,** TEM images of DNP, DNPC and DNPC-αCD47 (scale bar: 200 nm). **H,** The UV spectrum of DNP, DNPC and CY-09; **I,** CY-09 release curve of DNPC, DNPC-αCD47 and free CY-09; **J,** Coomassie blue staining of SDS-PAGE gel electrophoresis (Lane1: DNP, Lane1: DNPC, Lane3: DNPC-αCD47, Lane 4: αCD47).

confirmed by co-localization of Lysotracker and nanoparticles by confocal microscopy. As shown in Fig. 3F, no significant co-localization was observed, indicating that the nanoparticle can escape from lysosomes into the cytoplasm. The lysosome escape function of DNPC-αCD47 protects CY-09 from being degraded by various digestive enzymes in lysosomes and improves the bioavailability of CY-09. The TEM images also illustrate this result as shown in Fig. 3E. These results indicate that DNPC-αCD47 can be rapidly taken up by macrophages through dopamine-mediated endocytosis and protects the drug CY-09 from being degraded in lysosomes.

2.3. *Inhibition of NLRP3 inflammasome activation in vitro*

The NLRP3 inflammasome has been implicated in various inflammatory diseases, including atherosclerosis, so the activation of the NLRP3 inflammasome should be strictly controlled. As shown in Fig. 1B, in atherosclerosis, NLRP3 was consistently upregulated in mouse atherosclerotic plaques compared to non-atherosclerotic vascular tissue. In this study, an NLRP3 inhibitor, CY-09, was encapsulated in nanoparticles to inhibit NLRP3 activation and reduce inflammation in atherosclerotic plaques. In vitro immunofluorescence staining of NLRP3 was performed after treatment with different nanoparticles as shown in Fig. 4A, and the semiquantitative analysis of the expression area is shown in Fig. 4B. From this result, DNP slightly reduced the expression of NLRP3 compared with the control group, which may be due to the dopamine-mediated inhibition of NLRP3. In the DNPC and DNPC-αCD47 groups, the expression areas of NLRP3 were significantly reduced due to the strong anti-inflammatory effect of CY-09. The inhibition of NLRP3 activation after treatment of DNPC and NPC-αCD47 was also confirmed by flow cytometry analysis (Fig. 4C and S1).

The NLRP3 inflammasome is a cytosolic protein complex composed of NLRP3, ASC, and caspase-1, and activation of the NLRP3 inflammasome promotes the maturation and release of several proinflammatory cytokines, such as interleukin-1β (IL-1β), and high expression of related proteins. In this study, IL-1β levels in supernatants from LPS-primed BMDMs treated with nanoparticles for 3 h and then stimulated with

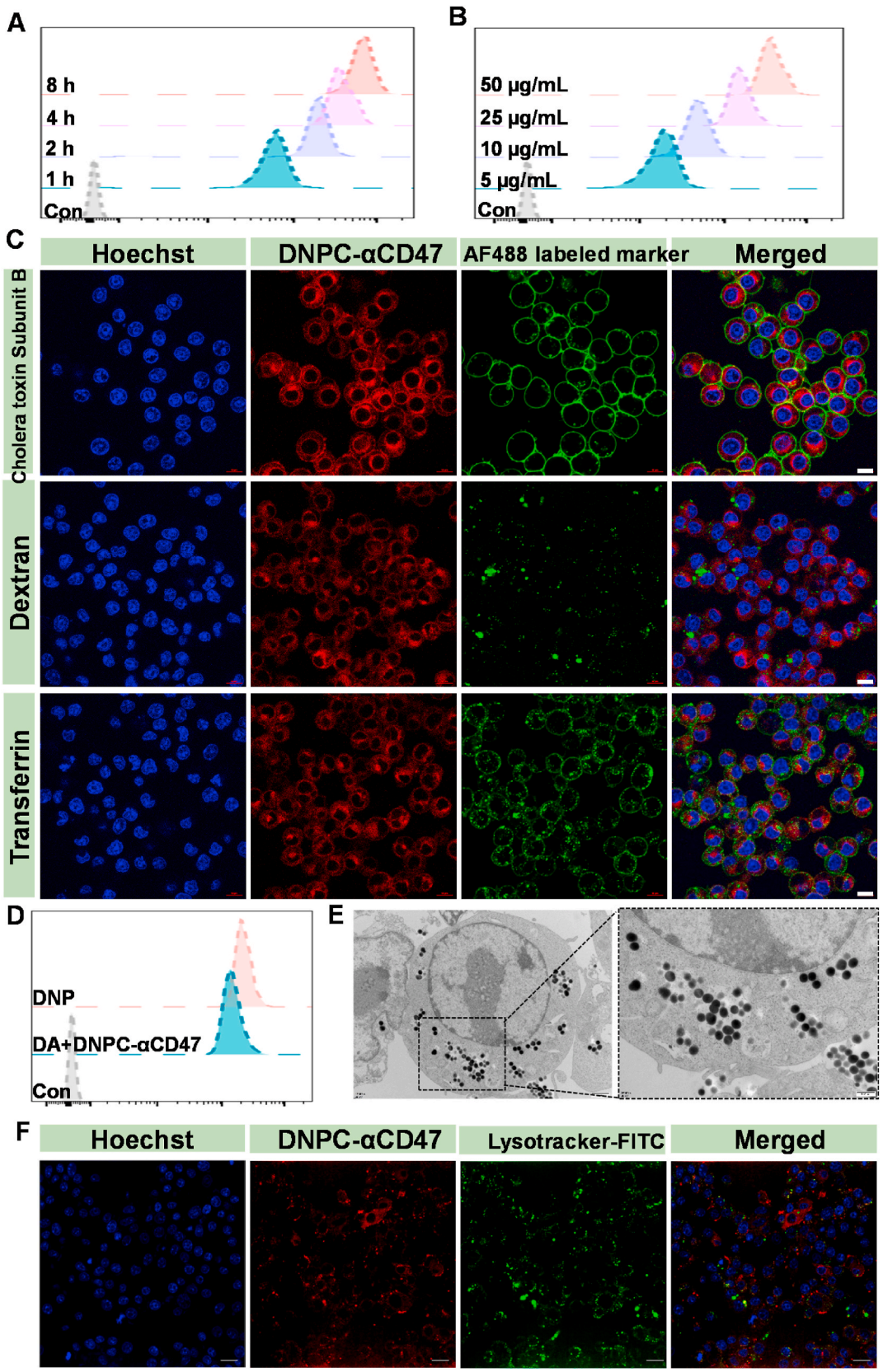

Fig. 3. **A-B,** Fluorescence intensity of macrophages after incubation with DNPC-αCD47 at different times or different concentrations. **C,** Endocytic pathway of DNPC-αCD47, indicating the composite nanomedicine was co-located with three different endocytic markers (Scale bar: 10 μm). **D,** Fluorescence intensity reduction of cells after incubation with free dopamine and nanoparticles. **E,** TEM images of macrophages uptake DNPC-αCD47 nanoparticles (Scale bar: 500 nm in enlarged image). **F,** Co-localization of DNPC-αCD47 and lysotracker (Scale bar: 10 μm).

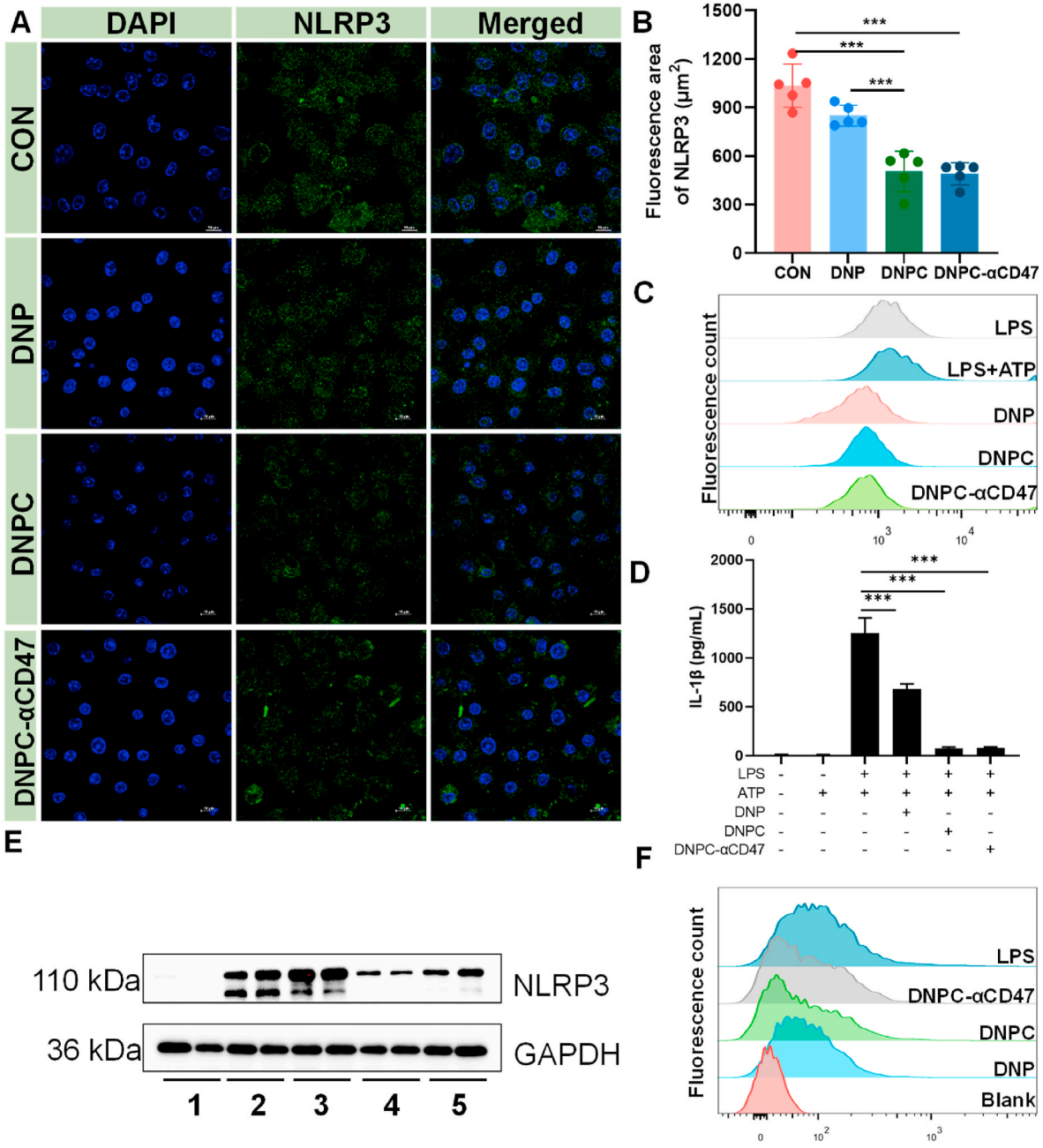

Fig. 4. A, Immunofluorescence staining of NLRP3 in BMDMs after treatment of DNP, DNPC and DNPC-αCD47 (Scale bar: 10 μm); **B,** Semi-quantitative analysis of expression area of NLRP3; **C,** Fluorescence intensity of NLRP3 after treatment by flow cytometer. **D,** ELISA of IL-1β in supernatants from LPS-primed BMDMs treated for 3 h with nanoparticles and then stimulated with ATP for 30 min; **E,** Expression of NLRP3 protein by Western blot (Lane1: Blank, Lane2: LPS + ATP, Lane3: LPS + ATP + DNP, Lane4: LPS + ATP + DNPC, Lane5: LPS + ATP + DNPC-αCD47). **F,** In vitro ROS reduction of macrophages detected by flow cytometer after treatment with nanoparticles.

ATP for 30 min were detected by enzyme-linked immunosorbent assay (ELISA). As shown in Fig. 4D, IL-1β levels were reduced after nanoparticle treatment. Specifically, CY-09 encapsulated in DNPC and DNPC-αCD47 groups significantly inhibited NLRP3 inflammasome activation and IL-1β release. The NLRP3 protein was also examined by Western blot. The expression of NLRP3 was significantly reduced after treatment with DNPC and DNPC-αCD47 (Fig. 4E and S2). Compared with the DNPC group, the expression of NLRP3 slightly increased in the DNPC-αCD47 group, perhaps because CD47 could ameliorate the production of NLRP3 inflammasome-induced IL-1β as mentioned above. In addition, dopamine is known to be a potent antioxidant and to protect neurocytes from oxidative stress by scavenging free radicals [32]. In this study, a reduction in ROS levels after nanoparticle treatment was also detected by flow cytometry (Fig. 4F). ROS scavenging plays an important role in regulating the microenvironment of macrophages. Taken together, the encapsulation of CY-09 significantly halts the activation of NLRP3 inflammasomes and reduces the release of IL-1β, and polydopamine-based nanoparticles can also scavenge intracellular ROS, thereby regulating the metabolic microenvironment.

2.4. Enhancement of efferocytosis and accumulation in plaques

In atherosclerosis, hyperlipidemia and hypercholesterolemia can induce apoptosis of macrophages and smooth muscle cells, leading to the accumulation of these apoptotic cells and debris within atherosclerotic plaques [33]. To prevent these apoptotic cells or debris from

causing inflammatory consequences, macrophages can recognize the "eat-me" signal on the surface of apoptotic cells and quickly and efficiently remove these cells through a phagocytic process known as programmed cell clearance or "efferocytosis" [34,35]. However, the "eat me" signaling axis can be blocked by anti-phagocytic "don't eat me" signals expressed on the cell surface (e.g. expression of CD47). CD47 is a key anti-phagocytic molecule, but a wide range of cancers upregulate CD47 [36]. As shown in Fig. 1A, in atherosclerosis, CD47 was consistently upregulated in mouse atherosclerotic plaques compared to non-atherosclerotic vascular tissue. Previous studies have reported that anti-CD47 antibody treatment significantly reduces atherosclerosis in the aortic sinus and aortic adventitia. In the present study, the anti-CD47 antibody was conjugated to the surface of DNPC nanoparticles to block antiphagocytic signaling. In vitro phagocytosis assays showed that DNPC-αCD47 was effective in inducing the clearance of diseased and apoptotic vascular SMCs and macrophages exposed to oxidized phospholipids, mimicking the atherosclerotic environment (Fig. 5A–B). In addition, chronic inflammation promotes increased permeability of the endothelial layer in atherosclerosis, allowing nanoparticles to accumulate. The enhanced permeability and retention (EPR) effect of the nanoscale delivery system can achieve a high degree of aggregation at the site of the atherosclerotic plaque and play a therapeutic role [9]. As shown in Fig. 5C and Figs. S3–4, the accumulation of Ce6-labeled DNPC-αCD47 nanoparticles was detected in the aorta compared to the saline group. Subsequently, flow cytometry showed that a greater percentage of Ly-6C^{hi} monocytes had taken up the nanoparticles in the atherosclerotic aorta after tail vein administration (Fig. 5D). From a mechanistic perspective, DNPC-αCD47 therapy was associated with

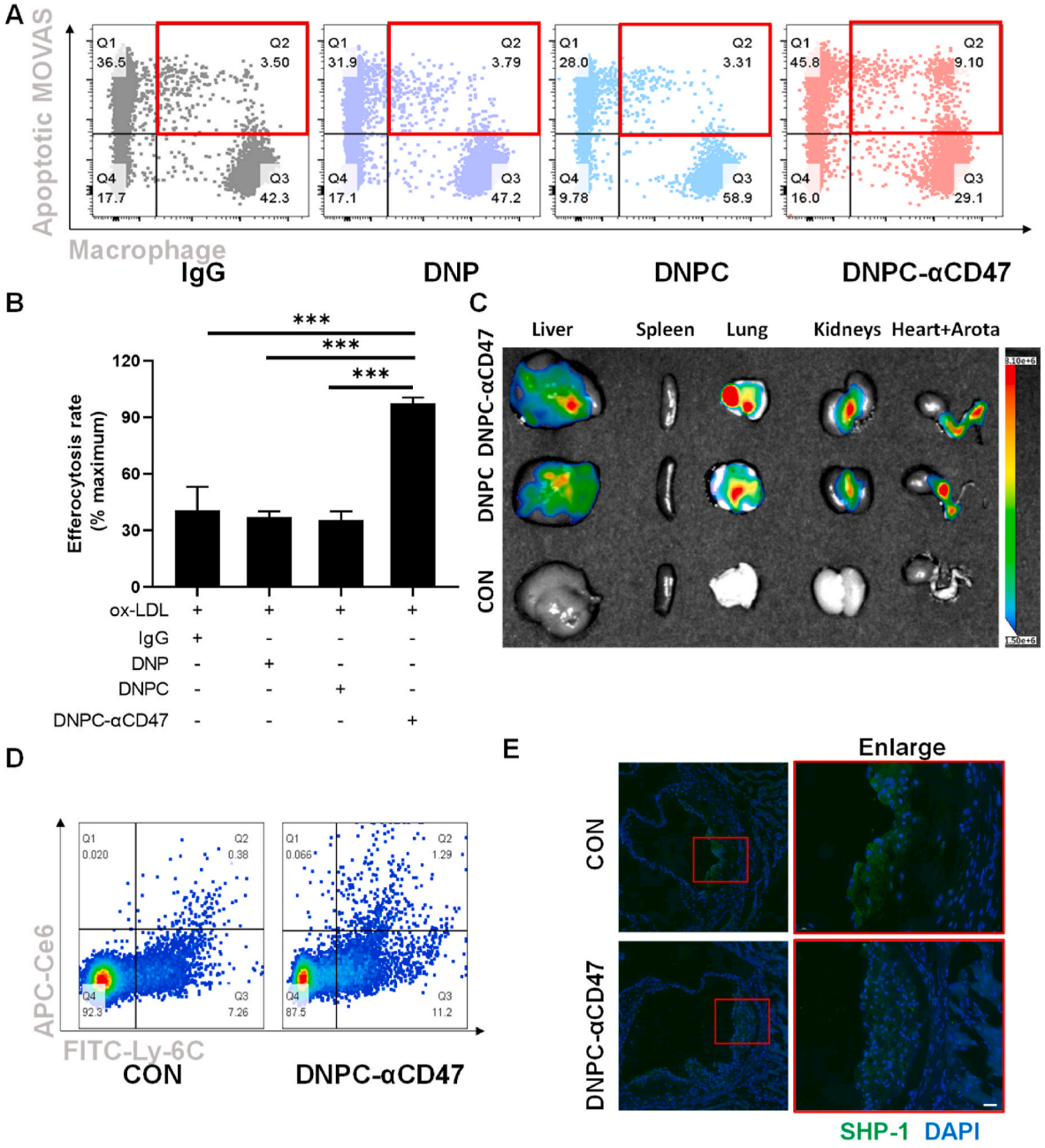

Fig. 5. A-B, DNPC-αCD47 promotes efferocytosis of MOVAS after exposure to pro-atherosclerotic lipids. **C,** Accumulation of Ce6 labeled nanoparticles in the aorta of the atherosclerotic mouse. **D,** Enhanced uptake is observed by Ly-6C^{hi} monocytes in the aorta. **E,** The immunofluorescence images of SHP-1, a key anti-phagocytic effector molecule known to signal downstream of CD47 (Scale bar: 20 μm).

marked suppression of intraplaque SHP-1 phosphorylation, confirming interruption of the anti-phagocytic signaling axis downstream of SIRPα, the cognate anti-phagocytic receptor of CD47 (Fig. 5E). Our findings reveal that DNPC-αCD47 nanoparticles specifically accumulate within atherosclerotic lesions and are subsequently phagocytosed by local macrophages. Importantly, the conjugated CD47 antibody on these nanoparticles impedes the anti-phagocytic signaling, thereby significantly enhancing the clearance of apoptotic cells within the lesions.

2.5. Prevention of atherosclerosis in vivo

To evaluate the therapeutic effect of nanoparticles on atherosclerosis, a chronic atherosclerosis model (Apoe$^{-/-}$ mice fed a high-fat 'Western' diet for 11 weeks) was established. Mice were divided into 4 groups and administrated with DNP, DNPC, DNPC-αCD47, and saline every three days for one month. After injection, mice were sacrificed, and blood and major organs were collected for analysis. Hearts were fixed in 4 % paraformaldehyde, dehydrated, and OCT-embedded for frozen sectioning. Masson trichrome staining of the aortic root was performed to analyze the necrotic core of traced lesions. As shown in Fig. 6A (left), compared to the other groups, mice treated with nanoparticles have a smaller necrotic core. After analysis, DNPC and DNPC-αCD47 significantly reduced the necrotic core area of plaque, and DNPC-αCD47 further decreased the necrotic core than DNPC treatment (Fig. 6C). Furthermore, compared to mice treated with saline (CON group), DNP, and DNPC, mice treated with DNPC-αCD47 develop significantly smaller atherosclerotic plaques as measured by Oil Red O (ORO) staining in the aortic sinus (Fig. 6A–B and Figs. S5–6). Similarly,

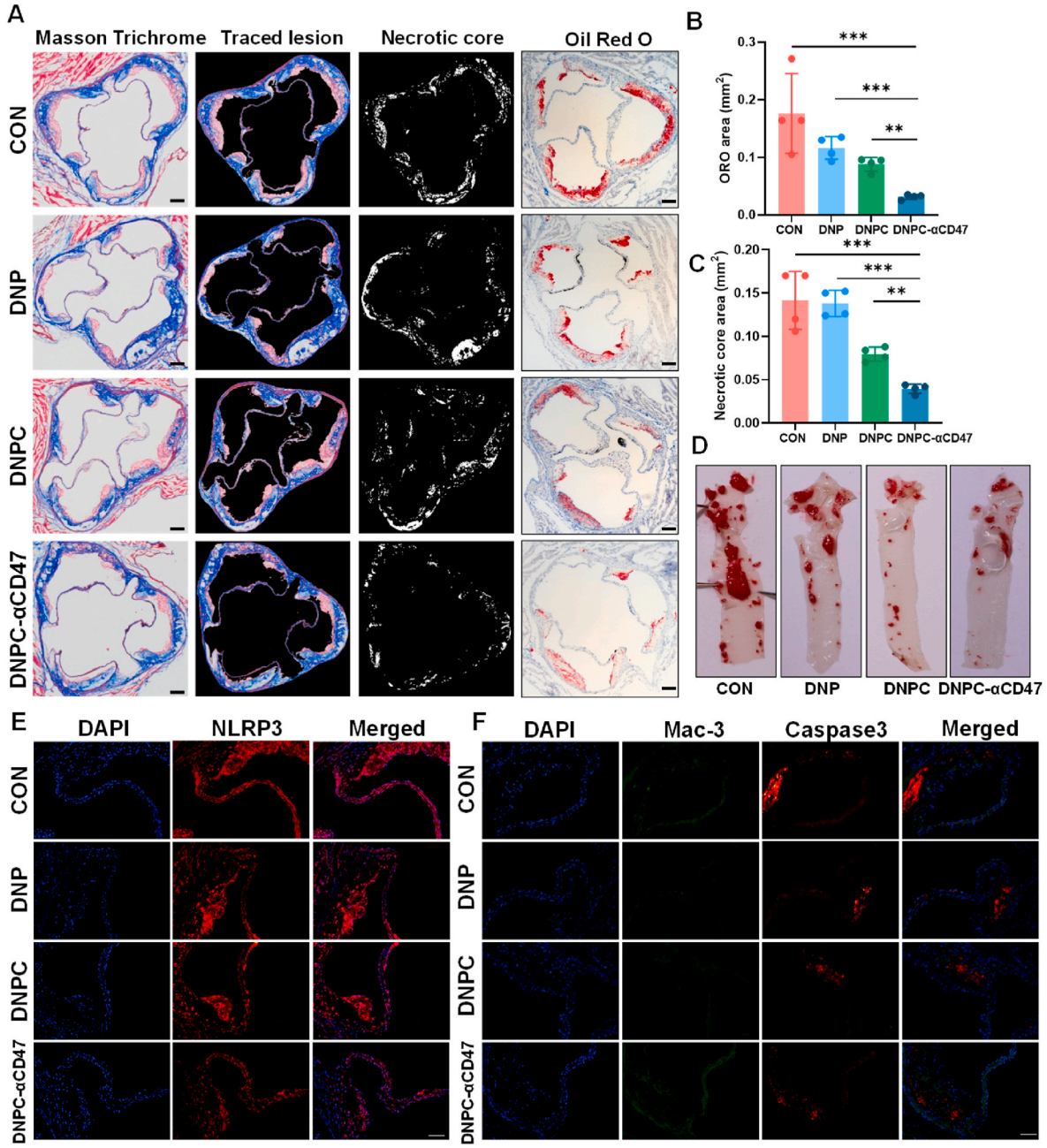

Fig. 6. A, Masson trichrome (left) and Oil red O (right) staining of aortic sinus after treatment of different nanoparticles (Scale bar: 100 μm). **B,** Oil red O staining of the aorta after treatment, total aortic atherosclerosis content is also reduced. **C-D,** Quantitative analysis of necrotic core area and ORO area of aortic sinus. **E-F,** Immunofluorescence of NLRP3, Mac-3 and cleaved caspase-3 in aortic sinus after different treatments (Scale bar: 50 μm).

DNPC-αCD47 nanoparticle treatment has a better effect than DNPC nanoparticles. Moreover, tissue ORO staining of the aorta also showed similar results (Fig. 6D). To observe the anti-inflammation effect of these nanoparticles, NLRP3 was stained in the aortic sinus by immunofluorescence. As expected, the expression of NLRP3 is lower in mice treated with DNPC and DNPC-αCD47 than in other groups (Fig. 6E). From the results, DNPC nanoparticles encapsulated with CY-09 also prevent the inflammatory response and necrotic core compared to the DNP and CON groups. In addition, to investigate efferocytosis in vivo, lesions were stained for SHP-1 phosphorylation and Mac-3. Apoptotic cells stained with cleaved caspase-3 were significantly lower in DNPC-αCD47-treated mice than in the other groups. The ratio of free to macrophage-associated apoptotic cells was lower in lesions from DNPC-αCD47 animals, indicating increased efferocytic activity in the vascular bed (Fig. 6F). Intraplaque SHP-1 phosphorylation was also observed in nanoparticle-treated mice, suggesting that antiphagocytic signaling downstream of CD47-SIRPα.

2.6. Single-cell RNA sequencing reveals an anti-inflammatory signature

To assess the regulation of the intra-plaque microenvironment on lesions, large-scale single-cell RNA sequencing (scRNA-seq) was performed from the aorta after being treated with DNPC-αCD47 (Fig. 7A). After quality control and filtering, about 26,915 cells from the control and 29,598 cells from the DNPC-αCD47 group were included in the scRNA-seq analysis (Fig. S7 and Table S2). Gene expression data from

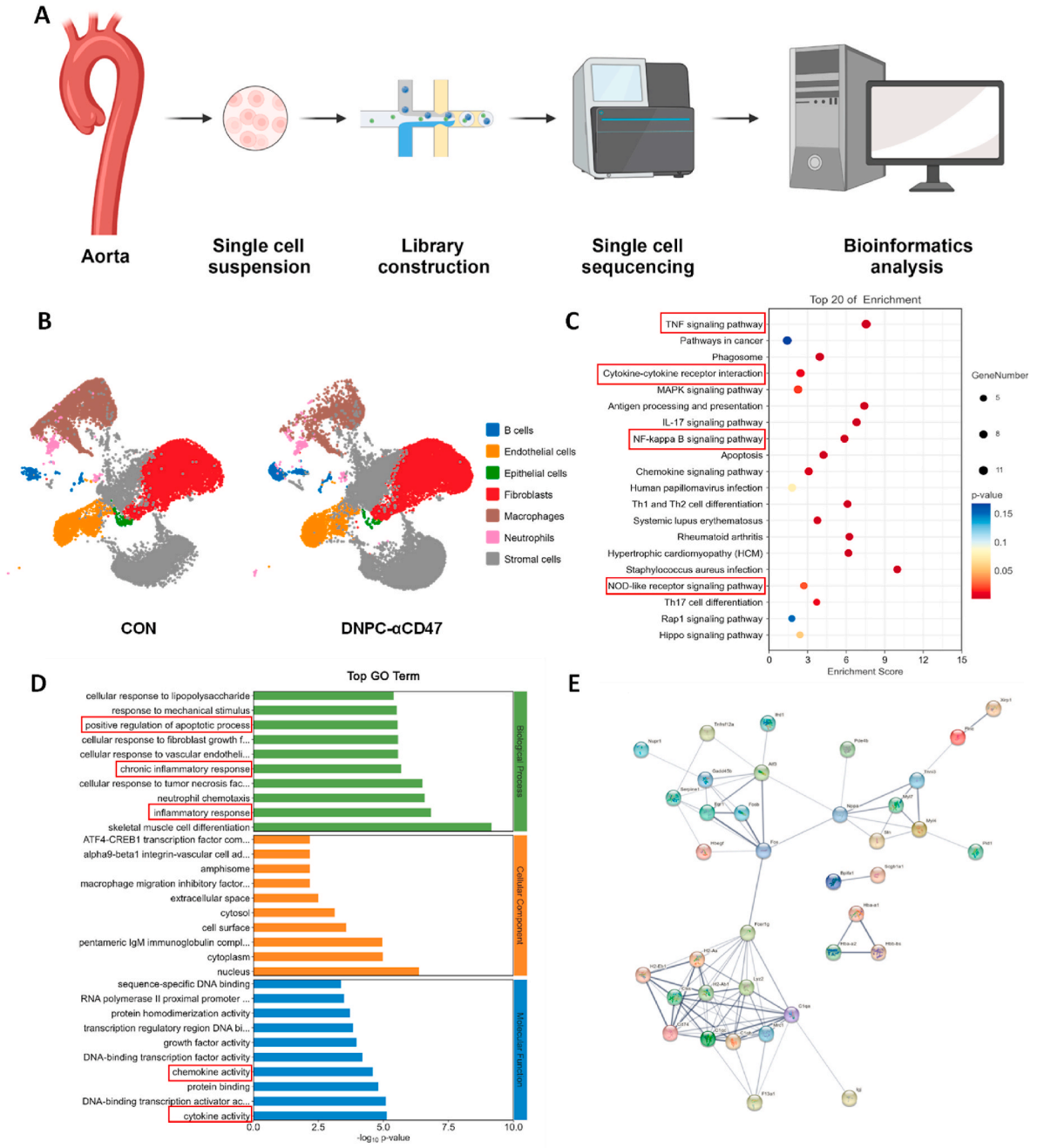

Fig. 7. A, Workflow for single-cell RNA-seq (Created with Biorender.com); **B,** Unsupervised dimensionality reduction identifies 7 major immune-related cell types with a similar gene expression (n = 3 biologically independent animals per group); **C,** The KEGG enrichment of downregulated gene expression; **D,** The GO enrichment and pathway analysis of differential gene expression; **E,** Up-down regulation of Top25 differentially expressed gene interaction network.

cells extracted from both conditions were aligned and projected in a 2-dimensional space through t-stochastic neighbor embedding (t-SNE) to allow identification of overlapping and atherosclerosis-associated immune cell populations (Fig. 7B and Fig. S8). Unsupervised Seurat-based clustering (see Methods section) singled out 7 distinct cell clusters (including B cells, Endothelial cells, Epithelial cells, Fibroblasts, Macrophages, Neutrophils, and Stromal cells) (Fig. 7B and Fig. S9). We found that DNPC-αCD47 elicited numerous changes in lesional macrophages, which included a decrease in pro-inflammatory transcripts (Ccl6, Ccl8, Ccl9, and Pf4) (Table S3).

The KEGG functional enrichment analyses also revealed that DNPC-αCD47 induced a decreased signature in inflammation-related TNF signaling pathway, cytokine-cytokine receptor interaction, NF-κB singling pathway, and NOD-like receptor signaling pathway (Fig. 7C and Fig. S10). Interestingly, gene ontology (GO) enrichment analysis further showed that macrophages downregulated genes implicated in inflammatory response and neutrophil chemotaxis (Fig. 7D and Fig. S11).

2.7. Safety assessment of bifunctional nanoparticles

Lately, a formal assessment has been conducted to evaluate the safety of nanoparticles. The body weight of mice was recorded during treatment, as illustrated in Fig. 8A, and no significant loss in body weight was observed across all groups. Furthermore, after treatment, blood routine analysis was performed on the mice (Fig. 8B–D). As illustrated in Fig. 8B, the white blood cell count decreased in the DNPC and DNPC-αCD47 groups, although the results were not statistically significant. It is worth noting that treatment with DNPC-αCD47 did not result in anemia, which is a major complication that hinders the translation of pro-efferocytic antibodies (Fig. 8D). Additionally, the serum biochemical analysis indicates a slight decrease in cholesterol, low-density lipoprotein, and triglyceride levels with DNPC-αCD47 treatment, but the results were not statistically significant. The underlying mechanisms require further investigation in future studies. H&E staining of tissue sections revealed normal major organs and no histopathological abnormalities, indicating no signs of cell or tissue damage in vivo from these nanoparticles (Fig. S12). Given that DNPC-αCD47 treatment did not demonstrate any of these potential toxicities, these data are consistent with the ability of nanoparticles to avoid off-target effects due to their specific accumulation within macrophages.

3. Conclusion

Atherosclerosis is a chronic inflammatory disease characterized by macrophage dysfunction, contributing significantly to plaque development. As shown in Fig. 1A–B, high expression of CD47 and NLRP3 was detected in atherosclerotic plaque, underlining the role of inflammatory reactions and macrophage-mediated phagocytosis in this context. Despite advances in the development of drugs that can modulate lesional inflammation and/or reactivate apoptotic debris engulfment in the necrotic core, single-agent therapies often fall short of effectively suppressing plaque formation. To address these limitations, we have engineered polydopamine-based nanoparticles that encapsulate an NLRP3 inhibitor and are conjugated with anti-CD47 antibodies, offering multifunctional regulation of macrophages. Notably, this nanoparticle can be prepared and functioned with a simple method, without requiring complicated synthesis and fabrication processes. Our in vitro studies demonstrate that these nanoparticles effectively inhibit NLRP3 expression and block the anti-phagocytic signals. Furthermore, in vivo studies in animal models show a significant reduction in plaque burden without inducing toxicity. Moreover, scRNA-seq data suggests a suppression of cytokine-dependent vascular inflammation by these nanoparticles. To summarize, our study advocates a novel synergistic therapeutic strategy using anti-CD47 conjugated bifunctional nanoparticles. This approach effectively modulates the plaque microenvironment at both intracellular and extracellular levels.

4. Experiment section

The Supporting Information includes details on the materials, methods, preparation, and characterization of the bifunctional nanoparticle conjugated with anti-CD47, as well as in vitro and in vivo studies, their respective mechanisms, and statistical analysis.

Conflict of interest

Zhiyong Qian is an editorial board member for Bioactive Materials and was not involved in the editorial review or the decision to publish this article. All authors declare that there are no competing interests. The authors declare that they have no known competing financial interests or personal relationships that could have appeared to influence

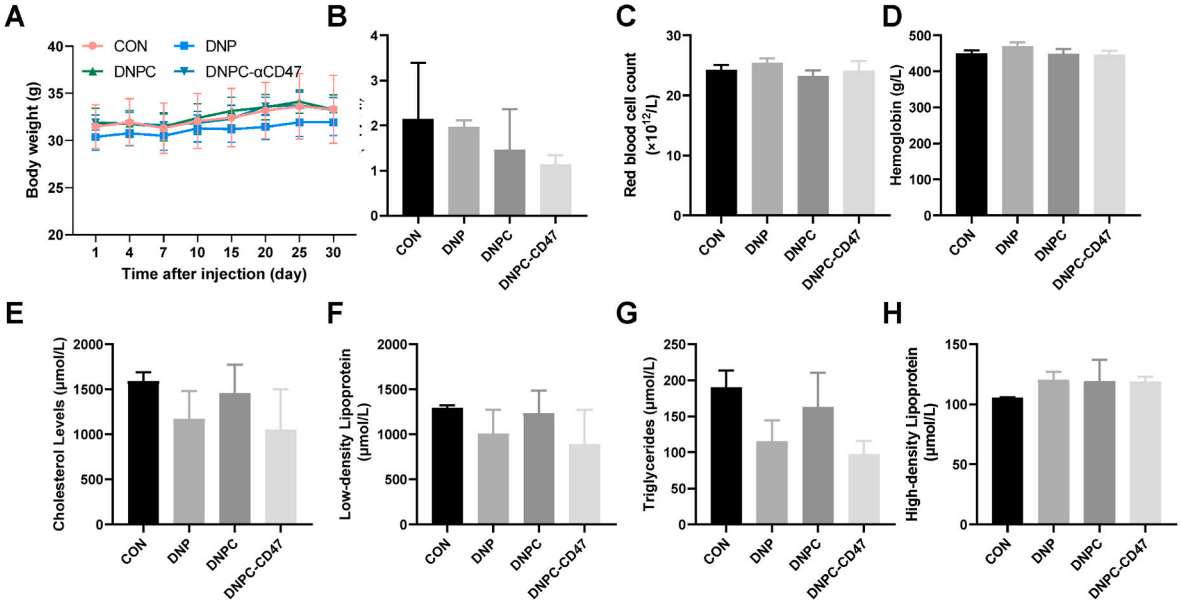

Fig. 8. A, Body weight shift of mice treated with nanoparticles. **B-D,** blood routine analysis of mice after treatments. **E-H,** Serum biochemical analysis of mice after treatments.

the work reported in this paper.

CRediT authorship contribution statement

Qiang Luo: Writing – original draft, Methodology, Investigation, Funding acquisition, Formal analysis, Data curation. **Liqun Dai:** Writing – original draft, Methodology, Data curation. **Junli Li:** Resources, Funding acquisition, Formal analysis. **Heyanni Chen:** Writing – review & editing, Data curation. **Ying Hao:** Methodology, Funding acquisition. **Qing Li:** Software. **Lili Pan:** Writing – review & editing, Investigation, Data curation. **Chengxiang Song:** Software. **Zhiyong Qian:** Supervision. **Mao Chen:** Supervision, Funding acquisition.

Declaration of competing interest

The authors declare no conflict of interest.

Acknowledgments

Qiang Luo and Liqun Dai contributed equally to this work. This work was supported by the National Natural Science Foundation of China (82202310, 82170375 and 11902211); Key Research and Development Project of Science & Technology Department of Sichuan Province (2022ZDZX0020); Nature Science Foundation of Sichuan Province (23NSFSC2409 and 2023NSFSC1339); 1·3·5 project for disciplines of excellence-Clinical Research Fund, West China Hospital, Sichuan University; China Postdoctoral Science Foundation (2022M712254); The Fundamental Research Funds for the Central Universities (20826041F4149); Post-Doctor Research Project, West China Hospital, Sichuan University (21HXBH068); The authors would like to thank Sisi Wu, Xiaojiao Wang, Dan Luo, Xin Luo and Yinchan Wang, (Research Core Facility, West China Hospital, Sichuan University) for their help in cell studies, histological studies and flow cytometer. This manuscript was completed by Qiang Luo and then modified by DeepL software (www.deepl.com).

Appendix A. Supplementary data

Supplementary data to this article can be found online at https://doi.org/10.1016/j.bioactmat.2023.12.024.

References

[1] C. Gao, Q. Huang, C. Liu, C.H.T. Kwong, L. Yue, J.-B. Wan, S.M.Y. Lee, R. Wang, Treatment of atherosclerosis by macrophage-biomimetic nanoparticles via targeted pharmacotherapy and sequestration of proinflammatory cytokines, Nat. Commun. 11 (2020) 2622, https://doi.org/10.1038/s41467-020-16439-7.

[2] N. Leitinger, I.G. Schulman, Phenotypic polarization of macrophages in atherosclerosis, Arterioscler. Thromb. Vasc. Biol. 33 (2013) 1120–1126, https://doi.org/10.1161/ATVBAHA.112.300173.

[3] D. Karunakaran, M. Geoffrion, L. Wei, W. Gan, L. Richards, P. Shangari, E. M. DeKemp, R.A. Beanlands, L. Perisic, L. Maegdefessel, U. Hedin, S. Sad, L. Guo, F. D. Kolodgie, R. Virmani, T. Ruddy, K.J. Rayner, Targeting macrophage necroptosis for therapeutic and diagnostic interventions in atherosclerosis, Sci. Adv. 2 (2016) e1600224, https://doi.org/10.1126/sciadv.1600224.

[4] O. Soehnlein, P. Libby, Targeting inflammation in atherosclerosis — from experimental insights to the clinic, Nat. Rev. Drug Discov. 20 (2021) 589–610, https://doi.org/10.1038/s41573-021-00198-1.

[5] E.A. Van Vré, H. Ait-Oufella, A. Tedgui, Z. Mallat, Apoptotic cell death and efferocytosis in atherosclerosis, Arterioscler. Thromb. Vasc. Biol. 32 (2012) 887–893, https://doi.org/10.1161/ATVBAHA.111.224873.

[6] Y. Kojima, J.-P. Volkmer, K. McKenna, M. Civelek, A.J. Lusis, C.L. Miller, D. Direnzo, V. Nanda, J. Ye, A.J. Connolly, E.E. Schadt, T. Quertermous, P. Betancur, L. Maegdefessel, L.P. Matic, U. Hedin, I.L. Weissman, N.J. Leeper, CD47-blocking antibodies restore phagocytosis and prevent atherosclerosis, Nature 536 (2016) 86–90, https://doi.org/10.1038/nature18935.

[7] S. Gholamin, S.S. Mitra, A.H. Feroze, J. Liu, S.A. Kahn, M. Zhang, R. Esparza, C. Richard, V. Ramaswamy, M. Remke, A.K. Volkmer, S. Willingham, A. Ponnuswami, A. McCarty, P. Lovelace, T.A. Storm, S. Schubert, G. Hutter, C. Narayanan, P. Chu, E.H. Raabe, G. Harsh, M.D. Taylor, M. Monje, Y.-J. Cho, R. Majeti, J.P. Volkmer, P.G. Fisher, G. Grant, G.K. Steinberg, H. Vogel, M. Edwards, I.L. Weissman, S.H. Cheshier, Disrupting the CD47-SIRPα anti-phagocytic axis by a humanized anti-CD47 antibody is an efficacious treatment for malignant pediatric brain tumors, Sci. Transl. Med. 9 (2017) eaaf2968, https://doi.org/10.1126/scitranslmed.aaf2968.

[8] Y. Kojima, N. Werner, J. Ye, V. Nanda, N. Tsao, Y. Wang, A.M. Flores, C.L. Miller, I. Weissman, H. Deng, B. Xu, R.L. Dalman, S.M. Eken, J. Pelisek, Y. Li, L. Maegdefessel, N.J. Leeper, Proefferocytic therapy promotes transforming growth factor-β signaling and prevents Aneurysm formation, Circulation 137 (2018) 750–753, https://doi.org/10.1161/CIRCULATIONAHA.117.030389.

[9] G. Q, Z. Y, H. C, H. X, Z. H, X. X, T. J, L. Y, D. Y, L. J, W. C, G. Z, Y. Y, C. X, Blockade of CD47 ameliorates autoimmune inflammation in CNS by suppressing IL-1-triggered infiltration of pathogenic Th17 cells, J. Autoimmun. 69 (2016), https://doi.org/10.1016/j.jaut.2016.03.002.

[10] Y. Cui, H. Yu, Z. Bu, L. Wen, L. Yan, J. Feng, Focus on the role of the NLRP3 inflammasome in multiple sclerosis: pathogenesis, diagnosis, and therapeutics, Front. Mol. Neurosci. 15 (2022) 894298, https://doi.org/10.3389/fnmol.2022.894298.

[11] K.J. Moore, I. Tabas, Macrophages in the pathogenesis of atherosclerosis, Cell 145 (2011) 341–355.

[12] P. Libby, P.M. Ridker, A. Maseri, Inflammation and atherosclerosis, Circulation 105 (2002) 1135–1143, https://doi.org/10.1161/hc0902.104353.

[13] P. Duewell, H. Kono, K.J. Rayner, C.M. Sirois, G. Vladimer, F.G. Bauernfeind, G. S. Abela, L. Franchi, G. Nuñez, M. Schnurr, NLRP3 inflammasomes are required for atherogenesis and activated by cholesterol crystals, Nature 464 (2010) 1357–1361.

[14] K.V. Swanson, M. Deng, J.P.-Y. Ting, The NLRP3 inflammasome: molecular activation and regulation to therapeutics, Nat. Rev. Immunol. 19 (2019) 477–489, https://doi.org/10.1038/s41577-019-0165-0.

[15] Z. Duan, Q. Luo, X. Dai, X. Li, L. Gu, H. Zhu, X. Tian, H. Zhang, Q. Gong, Z. Gu, K. Luo, Synergistic therapy of a naturally inspired glycopolymer-based biomimetic nanomedicine harnessing tumor genomic instability, Adv. Mater. Deerfield Beach Fla. 33 (2021) e2104594, https://doi.org/10.1002/adma.202104594.

[16] H. Li, Q. Luo, H. Zhang, X. Ma, Z. Gu, Q. Gong, K. Luo, Nanomedicine embraces cancer radio-immunotherapy: mechanism, design, recent advances, and clinical translation, Chem. Soc. Rev. 52 (2023) 47–96, https://doi.org/10.1039/d2cs00437b.

[17] Q. Luo, L. Lin, Q. Huang, Z. Duan, L. Gu, H. Zhang, Z. Gu, Q. Gong, K. Luo, Dual stimuli-responsive dendronized prodrug derived from poly(oligo-(ethylene glycol) methacrylate)-based copolymers for enhanced anti-cancer therapeutic effect, Acta Biomater. 143 (2022) 320–332, https://doi.org/10.1016/j.actbio.2022.02.033.

[18] Q. Luo, Z. Duan, X. Li, L. Gu, L. Ren, H. Zhu, X. Tian, R. Chen, H. Zhang, Q. Gong, Z. Gu, K. Luo, Branched polymer-based redox/enzyme-activatable photodynamic nanoagent to trigger STING-dependent immune responses for enhanced therapeutic effect, Adv. Funct. Mater. 32 (2022) 2110408, https://doi.org/10.1002/adfm.202110408.

[19] Y. Kanthi, A. de la Zerda, B. Ronain Smith, Nanotherapeutic shots through the heart of plaque, ACS Nano 14 (2020) 1236–1242, https://doi.org/10.1021/acsnano.0c00245.

[20] T.J. Beldman, M.L. Senders, A. Alaarg, C. Pérez-Medina, J. Tang, Y. Zhao, F. Fay, J. Deichmöller, B. Born, E. Desclos, N.N. van der Wel, R.A. Hoebe, F. Kohen, E. Kartvelishvily, M. Neeman, T. Reiner, C. Calcagno, Z.A. Fayad, M.P.J. de Winther, E. Lutgens, W.J.M. Mulder, E. Kluza, Hyaluronan nanoparticles selectively target plaque-associated macrophages and improve plaque stability in atherosclerosis, ACS Nano 11 (2017) 5785–5799, https://doi.org/10.1021/acsnano.7b01385.

[21] S. Barua, S. Mitragotri, Challenges associated with penetration of nanoparticles across cell and tissue barriers: a review of current status and future prospects, Nano Today 9 (2014) 223–243, https://doi.org/10.1016/j.nantod.2014.04.008.

[22] C. Qiu, F. Xia, J. Zhang, Q. Shi, Y. Meng, C. Wang, H. Pang, L. Gu, C. Xu, Q. Guo, J. Wang, Advanced strategies for overcoming endosomal/lysosomal barrier in nanodrug delivery, Research 6 (2023) 148, https://doi.org/10.34133/research.0148.

[23] M.J. Mitchell, M.M. Billingsley, R.M. Haley, M.E. Wechsler, N.A. Peppas, R. Langer, Engineering precision nanoparticles for drug delivery, Nat. Rev. Drug Discov. 20 (2021) 101–124, https://doi.org/10.1038/s41573-020-0090-8.

[24] Z. Liu, H. He, Synthesis and applications of boronate affinity materials: from class selectivity to biomimetic specificity, Acc. Chem. Res. 50 (2017) 2185–2193, https://doi.org/10.1021/acs.accounts.7b00179.

[25] R. Wang, C. Yin, C. Liu, Y. Sun, P. Xiao, J. Li, S. Yang, W. Wu, X. Jiang, Phenylboronic acid modification augments the lysosome escape and antitumor efficacy of a cylindrical polymer brush-based prodrug, J. Am. Chem. Soc. 143 (2021) 20927–20938, https://doi.org/10.1021/jacs.1c09741.

[26] Z. Wang, Y. Xie, Y. Li, Y. Huang, L.R. Parent, T. Ditri, N. Zang, J.D. Rinehart, N. C. Gianneschi, Tunable, metal-loaded polydopamine nanoparticles analyzed by magnetometry, Chem. Mater. 29 (2017) 8195–8201, https://doi.org/10.1021/acs.chemmater.7b02262.

[27] C. Zhan, G. Lin, Y. Huang, Z. Wang, F. Zeng, S. Wu, A dopamine-precursor-based nanoprodrug for in-situ drug release and treatment of acute liver failure by inhibiting NLRP3 inflammasome and facilitating liver regeneration, Biomaterials 268 (2021) 120573, https://doi.org/10.1016/j.biomaterials.2020.120573.

[28] Y. Zou, X. Chen, P. Yang, G. Liang, Y. Yang, Z. Gu, Y. Li, Regulating the absorption spectrum of polydopamine, Sci. Adv. 6 (2020) eabb4696, https://doi.org/10.1126/sciadv.abb4696.

[29] Y. Fu, J. Zhang, Y. Wang, J. Li, J. Bao, X. Xu, C. Zhang, Y. Li, H. Wu, Z. Gu, Reduced polydopamine nanoparticles incorporated oxidized dextran/chitosan hybrid hydrogels with enhanced antioxidative and antibacterial properties for accelerated wound healing, Carbohydr. Polym. 257 (2021) 117598, https://doi.org/10.1016/j.carbpol.2020.117598.

[30] H. Gholami Derami, P. Gupta, K.-C. Weng, A. Seth, R. Gupta, J.R. Silva, B. Raman, S. Singamaneni, Reversible photothermal modulation of electrical activity of excitable cells using polydopamine nanoparticles, Adv. Mater. Deerfield Beach Fla. 33 (2021) e2008809, https://doi.org/10.1002/adma.202008809.

[31] J. Sun, Z. Wan, J. Xu, Z. Luo, P. Ren, B. Zhang, D. Diao, Y. Huang, S. Li, Tumor size-dependent abscopal effect of polydopamine-coated all-in-one nanoparticles for immunochemo-photothermal therapy of early- and late-stage metastatic cancer, Biomaterials 269 (2021) 120629, https://doi.org/10.1016/j.biomaterials.2020.120629.

[32] C. Iuga, J.R. Alvarez-Idaboy, A. Vivier-Bunge, ROS initiated oxidation of dopamine under oxidative stress conditions in aqueous and lipidic environments, J. Phys. Chem. B 115 (2011) 12234–12246, https://doi.org/10.1021/jp206347u.

[33] M.F. Linton, P.G. Yancey, S.S. Davies, W.G. Jerome, E.F. Linton, W.L. Song, A. C. Doran, K.C. Vickers, The role of lipids and lipoproteins in atherosclerosis, in: K. R. Feingold, B. Anawalt, M.R. Blackman, A. Boyce, G. Chrousos, E. Corpas, W.W. de Herder, K. Dhatariya, K. Dungan, J. Hofland, S. Kalra, G. Kaltsas, N. Kapoor, C. Koch, P. Kopp, M. Korbonits, C.S. Kovacs, W. Kuohung, B. Laferrère, M. Levy, E. A. McGee, R. McLachlan, M. New, J. Purnell, R. Sahay, A.S. Shah, F. Singer, M. A. Sperling, C.A. Stratakis, D.L. Trence, D.P. Wilson (Eds.), Endotext, MDText.com, Inc., South Dartmouth (MA), 2000. http://www.ncbi.nlm.nih.gov/books/NBK343489/. (Accessed 7 September 2023).

[34] A.M. Flores, N. Hosseini-Nassab, K.-U. Jarr, J. Ye, X. Zhu, R. Wirka, A.L. Koh, P. Tsantilas, Y. Wang, V. Nanda, Y. Kojima, Y. Zeng, M. Lotfi, R. Sinclair, I. L. Weissman, E. Ingelsson, B.R. Smith, N.J. Leeper, Pro-efferocytic nanoparticles are specifically taken up by lesional macrophages and prevent atherosclerosis, Nat. Nanotechnol. 15 (2020) 154–161, https://doi.org/10.1038/s41565-019-0619-3.

[35] G. Andrejeva, B.J. Capoccia, R.R. Hiebsch, M.J. Donio, I.M. Darwech, R.J. Puro, D. S. Pereira, Novel SIRPα antibodies that induce single-agent phagocytosis of tumor cells while preserving T cells, J. Immunol. 206 (2021) 712–721, https://doi.org/10.4049/jimmunol.2001019.

[36] Z. Bian, L. Shi, Y.-L. Guo, Z. Lv, C. Tang, S. Niu, A. Tremblay, M. Venkataramani, C. Culpepper, L. Li, Z. Zhou, A. Mansour, Y. Zhang, A. Gewirtz, K. Kidder, K. Zen, Y. Liu, Cd47-Sirpα interaction and IL-10 constrain inflammation-induced macrophage phagocytosis of healthy self-cells, Proc. Natl. Acad. Sci. USA 113 (2016) E5434–E5443, https://doi.org/10.1073/pnas.1521069113.